Evaluating the Robustness of Activator-Inhibitor Models for Cluster Head Computation

Lidia Yamamoto[1], Daniele Miorandi[2]

[1] Data Mining and Theoretical Bioinformatics Team (FDBT)
Image Sciences, Computer Sciences and Remote Sensing Laboratory (LSIIT)
University of Strasbourg, France
lidia.yamamoto@unistra.fr
[2] Pervasive Team, CREATE-NET, Trento, Italy
daniele.miorandi@create-net.org

Abstract. Activator-inhibitor models have been widely used to explain several morphogenetic processes. They have also been used to engineer algorithms for computer graphics, distributed systems and networks. These models are known to be robust to perturbations such as the removal of peaks of chemicals. However little has been reported about their actual quantitative performance under such disruptions.
In this paper we experimentally evaluate the robustness of two well-known activator-inhibitor models in the presence of attacks that remove existing activator peaks. We focus on spot patterns used as distributed models for cluster head computation, and on their potential implementation in chemical computing. For this purpose we derive the corresponding chemical reactions, and simulate the system deterministically.
Our results show that there is a trade-off between both models. The chemical form of the first one, the Gierer-Meinhardt model, is slow to recover due to the depletion of a required catalyst. The second one, the Activator-Substrate model, recovers more quickly but is also more dynamic as peaks may slowly move. We discuss the implications of these findings when engineering algorithms based on morphogenetic models.

1 Introduction

An activator-inhibitor model is a special case of a reaction-diffusion system where two chemicals interact in an antagonistic way, resulting in Turing patterns in space [1], such as spots and stripes on the skin of animals (e.g. leopard, zebra).

Activator-inhibitor models are recurrent components in morphogenesis. They offer an abstract model to explain many different morphogenetic phenomena, including the regular spacing of cactus thorns and bird feathers, shape regeneration after damage, the production of sequences of repeated elements such as insect body segments, the assembly of photoreceptor cells in insect eyes, and the positioning of leaves in growing plants [2–6]. They have also been used as inspiration for algorithms to produce textures and landscapes in computer graphics, and for autonomous, decentralized, distributed coordination algorithms, for instance in

pre-print of paper to appear in:
Marco Dorigo et al. (Eds.), Proceedings of the 7th International Conference on Swarm Intelligence (ANTS), Special Session on Morphogenetic Engineering, Brussels, Belgium, September 2010.
The original publication is available at www.springerlink.com

amorphous computing [7], wireless and sensor networks [8–10], and autonomous surveillance systems [11, 12].

It has been pointed out that activator-inhibitor models are robust to perturbations in the resulting patterns [3]. For instance, removing an activator peak results in this peak being regenerated or another peak being formed at a nearby place. However little has been reported about the actual quantitative performance of activator-inhibitor models under perturbations.

In this paper we experimentally evaluate the robustness of two well-known activator-inhibitor models in the presence of attacks that remove existing activator peaks. The first model is the well-known Gierer-Meinhardt Activator-Inhibitor Model and the second one is the Activator-Depleted Substrate Model. Both models are extensively described in [3, 6].

We focus on spot patterns (as opposed to stripes). Spots can be used to place differentiated functions at activator peaks, such as cluster heads in ad hoc and sensor networks [13–15]. Cluster heads can serve a variety of functions, such as aggregating information from nearby sensor nodes, or saving energy by switching off redundant nodes. The activator-inhibitor system used in this way can be regarded as a distributed algorithm that solves an instance of a cluster head election problem.

Instead of the traditional approach of directly integrating the reaction-diffusion equations provided, we derive the corresponding equations from chemical reactions using the law of mass action. The goal of this method is to ensure compatibility with a potential chemical implementation, either in an artificial chemistry [16, 17], or in natural chemical computing such as reaction-diffusion processors [18]. For this purpose, we reverse engineer both models from the equations back to the chemical reactions, and then simulate the resulting system deterministically by integrating the new set of equations obtained.

Our results show that the chemical derivation of the first model, the Gierer-Meinhardt model, seems not so robust as expected, since peaks of activator do not easily recover due to the depletion of a required catalyst. This catalyst does not appear in the original equations, but is necessary to achieve the desired inhibition effect. The second model evaluated, the Activator-Substrate model, is much faster at recovering from perturbations on activator peaks. On the other hand, it is also more dynamic, and peaks tend to change location sometimes. Therefore, there is a trade-off between both systems. We discuss the implications of these findings for engineering algorithms based on morphogenetic mechanisms.

2 Chemical Kinetics and Reaction-Diffusion Systems

The *Law of Mass Action* states that, in a well-stirred reactor, the average speed (or rate) of a chemical reaction is proportional to the product of the concentrations of its reactants [19].

The concentration dynamics of all molecules in the system can be described by a system of ordinary differential equations (ODE), where each equation describes the change in concentration of one particular molecular species. This

ODE system can be expressed in matrix notation as follows:

$$\frac{d\boldsymbol{c}}{dt} = \mathbf{M}\boldsymbol{v} \tag{1}$$

where $d\boldsymbol{c}/dt$ is the vector of differential equations for each of the species C_i (with concentration c_i), in the system; M is the stoichiometric matrix of the system; and $\boldsymbol{v}$ is a vector of rates for each reaction. The rates may follow the law of mass action as well as other laws such as enzyme and Hill kinetics.

A reaction-diffusion system is a chemical reaction system in which substances not only react but may also diffuse in space. It is expressed by a system of partial differential equations (PDE) describing the change in concentrations of substances caused by both reaction and diffusion effects combined:

$$\frac{\partial \mathbf{c}}{\partial t} = \mathbf{f}(\boldsymbol{c}) + D\nabla^2\boldsymbol{c} \tag{2}$$

The vector $\boldsymbol{c}$ now refers to the concentration level c_i of each chemical C_i at position (x, y) in space. The reaction term $\mathbf{f}(\boldsymbol{c})$ describes the reaction kinetics (like in Eq. (1), but now expressed for each point in space). The diffusion term $D\nabla^2\boldsymbol{c}$ tells how fast each chemical substance will diffuse in space. D is a diagonal matrix containing the diffusion coefficients, and ∇^2 is the Laplacian operator.

3 Activator-Inhibitor Models

Activation-inhibition models describe situations in which two competing processes take place over space and time. The first one (*short-range activation*) tends to self-enhance the process within the local neighbourhood. A competing force (*long-range inhibition*), weaker but with a longer spatial range, tends to decrease the activation effect in the surrounding space. Under certain conditions, the interaction between short-range activation and long-range inhibition can lead to the formation of asymmetric spatial patterns, such as spots and stripes resembling those found on the skin of animals. Alan Turing [1] was the first to present a mathematical model of morphogenesis based on reaction-diffusion dynamics, including activator-inhibitor dynamics.

In chemistry, activators and inhibitors are molecules that may diffuse over space. Activators trigger autocatalytic reactions that increase their own concentration (self-enhancement), but such effect has limited spatial range. On the other hand, activators also trigger inhibitory reactions that cause their own concentrations to decrease. Such a "negative impact" process has a reduced intensity when compared to self-enhancement, but has much larger spatial range.

Numerous alternative activator-inhibitor models are available in literature [1–4, 6]. They all achieve similar short-range activation and long-range inhibition effects, but differ in the chemicals needed, the way they interact, and the characteristics of the resulting patterns. In this paper we focus on two of these models: The Gierer-Meinhardt Activator-Inhibitor Model, and the Activator-Depleted Substrate Model, both from [3]. We describe them below.

3.1 The Gierer-Meinhardt Activator-Inhibitor Model

One of the most widely used activator-inhibitor model is named after Gierer and Meinhardt [3], and is described by the following reaction-diffusion equations:

$$\frac{\partial a}{\partial t} = \frac{\sigma a^2}{h} - \mu_a a + \rho_a + D_a \nabla^2 a \tag{3}$$

$$\frac{\partial h}{\partial t} = \sigma a^2 - \mu_h h + \rho_h + D_h \nabla^2 h \tag{4}$$

In this model, a represents the concentration of a short–range autocatalytic substance (activator A) and h the concentration of is its long-range antagonist H, the inhibitor.

The concentration a tends to self-enhance (growth proportional to σa^2), but such growth is slowed down by the inhibitor by a factor $1/h$. The inhibitor is produced by the molecular collision of two activator molecules, and this reaction contributes to its growth by a factor of σa^2. Further, both activator and inhibitor concentrations decay proportionally to their respective values. The constants μ_a and μ_h describe the rates at which each substance decays. The terms ρ_a and ρ_h represent a constant inflow of substances A and H respectively. Molecules can move across nearby cells following the concentration gradient, hence the diffusion terms $D_a \nabla^2 a$ and $D_h \nabla^2 h$, where D_a and D_h are constant diffusion coefficients.

An important condition for the formation of asymmetric patterns in this model is $D_h \gg D_a$ (the inhibitor diffuses much faster than the activator). Another condition is that $\mu_h > \mu_a$ (the inhibitor drains more quickly than the activator). A full mathematical description of the necessary and sufficient conditions for pattern formation in activator-inhibitor systems can be found in [4].

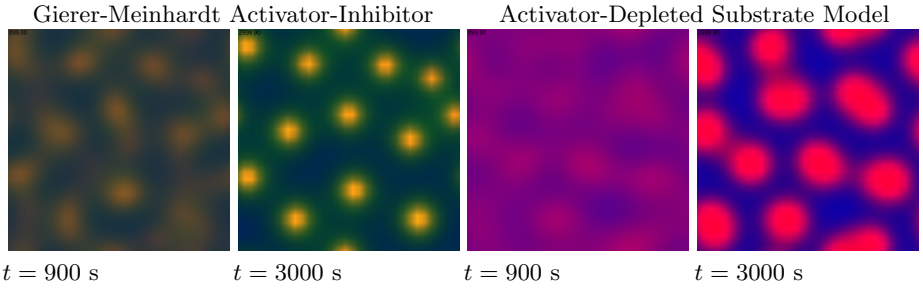

Fig. 1: Typical patterns resulting from the two activator-inhibitor models studied.

Figure 1 (left) illustrates the typical pattern formation process resulting from this activator-inhibitor model: starting from a homogeneous mix of chemicals that is slightly perturbed, the system progressively self-organizes into spot patterns, where the spots are regions of high activator concentration.

This model is widespread in literature [1–4, 6], but little has been discussed about its actual chemical implementation, either in natural or artificial chemistries. This is important if one would like to engineer reaction-diffusion systems using reaction-diffusion computers [18], or by evolving the corresponding chemical reaction graphs [20].

What set of chemical reactions can lead to equations (3) and (4)? Especially, the term $1/h$ in Eq. (3) does not seem to stem directly from mass action kinetics, neither from other well-known kinetic laws such as enzyme kinetics or Hill kinetics. In [2] it has been pointed out that the term $1/h$ comes from the effect of a third substance, a catalyst C, which is assumed to be in steady state.

Whereas an ODE system can be directly constructed from a system of chemical reactions, currently there is no firm and generic method to do the reverse operation, i.e. to derive the corresponding chemical reactions from a given ODE. We have reverse-engineered equations (3) and (4) using the catalyst hint from [2], and obtained the following result:

$$2A \xrightarrow{\sigma} 2A + H \quad (5)$$

$$A \xrightarrow{\mu_a} \emptyset \quad (6)$$

$$H \xrightarrow{\mu_h} \emptyset \quad (7)$$

$$\emptyset \xrightarrow{\rho_a} A \quad (8)$$

$$\emptyset \xrightarrow{\rho_h} H \quad (9)$$

$$C + 2A \xrightarrow{k_1} C + 3A \quad (10)$$

$$C + H \xrightarrow{k_2} H \quad (11)$$

$$C \xrightarrow{\mu_c} \emptyset \quad (12)$$

$$\emptyset \xrightarrow{\rho_c} C \quad (13)$$

Note that the first five reactions (5)-(9) stem directly from equations (3) and (4), while the other reactions (10)-(13) involve a "hidden" chemical C. C acts as a catalyst in the production of the activator A, however the inhibitor H consumes C, and it is the depletion of C through H that causes the inhibitory effect on A. This can be shown via the following analysis. We start by deriving the differential equations corresponding to the full set of reactions (5)-(13), using the Law of Mass Action:

$$\frac{da}{dt} = k_1 c a^2 - \mu_a a + \rho_a \quad (14)$$

$$\frac{dh}{dt} = \sigma a^2 - \mu_h h + \rho_h \quad (15)$$

$$\frac{dc}{dt} = -k_2 c h - \mu_c c + \rho_c \quad (16)$$

Eq. (15) corresponds directly to the reaction part of Eq. (4), so we do not need to look at it further. Now we focus on how to obtain the reaction part of Eq. (3) from Eqs. (14) and (16). For simplification we assume that $\mu_c = 0$, so that the inhibitor is the only responsible for a depletion of C. At steady state, the concentration of C stays stable, thus:

$$\frac{dc}{dt} = -k_2 c h + \rho_c = 0 \Rightarrow c = \frac{\rho_c}{k_2 h} \quad (17)$$

Substituting Eq. (17) in (14) we obtain:

$$\frac{da}{dt} = \frac{k_1 \rho_c a^2}{k_2 h} - \mu_a a + \rho_a \tag{18}$$

By setting $\sigma = k_1 \rho_c / k_2$ we obtain the reaction part of Eq. (3) as needed. Note therefore that Eq. (3) is only accurate when the system is in steady state. Perturbations may cause the catalyst concentrations to fluctuate, and therefore the approximation in Eq. (3) becomes a poor modelling of the system's dynamic behavior in these cases. This might partly account for the performance issues uncovered in our simulation experiments reported in Section 5.

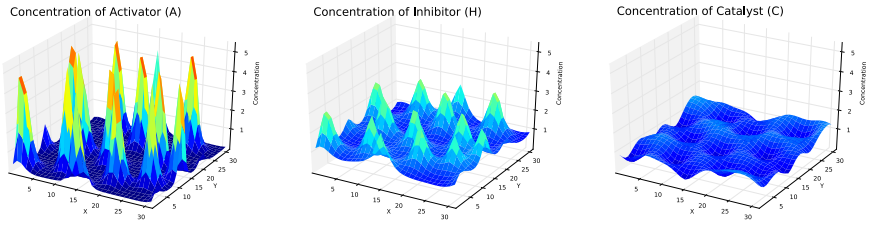

Fig. 2: Concentration levels of activator (left), inhibitor (center), and catalyst (right) for the Activator-Inhibitor pattern on Figure 1 (left) at $t = 3000$s.

Figure 2 shows the concentrations of activator, inhibitor and catalyst at the end of the simulation that generated Fig. 1 (left). We can see how the activator and inhibitor peaks coincide, the inhibitor peaks being more modest, while the catalyst valleys correspond to regions of high activator concentration.

3.2 Activator-Depleted Substrate Model

Several variations over the basic activator-inhibitor model have been proposed in the mathematical biology literature [3, 4, 21], some encompassing a larger number of equations, representing situations in which more complex interactions among molecules take place.

An interesting alternative approach in our context is the *activator-depleted substrate model* [3], or activator-substrate for short. Instead of modelling the explicit presence of a molecular species able to slow down the activation process, the activator-substrate model achieves a similar antagonistic effect through the depletion of a substrate S, which gets consumed during the production of the activator A. The resulting reaction-diffusion equations read:

$$\frac{\partial a}{\partial t} = \sigma_a s a^2 - \mu_a a + \rho_a + D_a \nabla^2 a \tag{19}$$

$$\frac{\partial s}{\partial t} = -\sigma_s s a^2 - \mu_s s + \rho_s + D_s \nabla^2 s \tag{20}$$

The substrate S gets consumed during the autocatalytic production of activator A. Both activator and substrate are produced everywhere at constant rate

ρ_a and ρ_s respectively, and decay at rate μ_a (resp. μ_s). Figure 1 (right) shows the typical pattern formation process using this model. Note that, in contrast to the previous model, here spots slowly change, and sometimes grow and divide, i.e. they can replicate. This behavior has been thoroughly studied in the Gray-Scott model [22], which is a special case of activator-substrate model.

Note that if it was not for the possibility to have different σ values for A and S (σ_a and σ_s), then it would have been straightforward to derive the corresponding chemical reactions. In order to allow for different σ_a and σ_s, we have come up with the following solution:

$$S + 2A \xrightarrow{\sigma_a} 3A \quad (21) \qquad \emptyset \xrightarrow{\rho_s} S \quad (24)$$

$$S + 2A \xrightarrow{k_s} 2A \quad (22) \qquad A \xrightarrow{\mu_a} \emptyset \quad (25)$$

$$\emptyset \xrightarrow{\rho_a} A \quad (23) \qquad S \xrightarrow{\mu_s} \emptyset \quad (26)$$

where $k_s = \sigma_s - \sigma_a$. With this we obtain the reaction part of Eqs. (19) and (20) from the law of mass action. Reactions (21) and (22) imply that, when two molecules of A and one of S react together, one extra molecule of A may be formed in some cases (reaction (21)), while in others (reaction (22)) the substrate molecule will simply be lost or degraded into something that can not be used by the system. So the second reaction can be seen as a kind of "error" or inefficiency in the process of autocatalysis of A, which can be nevertheless exploited to construct useful patterns.

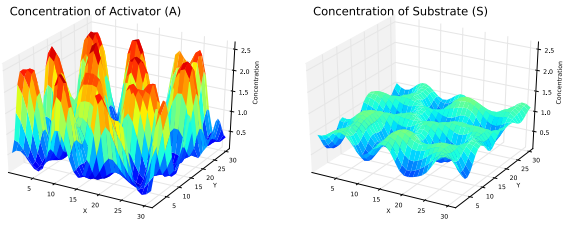

Fig. 3: Concentration levels of activator (left) and substrate (right) for the Activator-Substrate pattern on Figure 1 (right) at $t = 3000$s.

Figure 3 shows the concentrations of activator and substrate at the end of the simulation that generated Fig. 1 (right). The substrate valleys correspond to regions of high activator concentration. Note the wider and smoother activator peaks when compared to Fig. 2.

4 Experimental Setup

We compare the two models described in the previous section: the original Gierer-Meinhardt model (henceforth referred to as simply "activator-inhibitor"),

and the Activator-Depleted Substrate model (referred to as simply "activator-substrate"). We simulate a chemical implementation of both reaction-diffusion systems, according to their corresponding chemical reactions (5)-(13) and (21)-(26). This is in contrast to the traditional approach of integrating equations (3), (4), (19) and (20) directly.

We specify the chemical reactions, together with their rates, in a text format such as "`A + 2 B --> C , k=0.1`". Each line expresses a chemical reaction. The lines are then parsed, and the corresponding stoichiometric matrices are constructed, together with their reactant and product multisets. This information is then used to drive a generic integrator (based on the simple explicit Euler method) automatically, according to equations (1) and (2). This system is intuitive and versatile, and can simulate any kind of reaction-diffusion system with little effort. Besides ensuring chemical compatibility, another interest of such system is to make sure that the formula and behavior obtained stem directly from the chemical reactions, without hidden assumptions or simplifications. The visualization is performed with the help of the Breve simulator[3].

The parameters of the activator-inhibitor and activator-substrate models can be found in Table 1. Except for the extra coefficients k_i, all other constants are set to the same values as [6].

Activator-Inhibitor		
$\sigma = 0.02$	$\mu_a = 0.01$	$\rho_a = 0$
$k_1 = 0.01$	$\mu_h = 0.02$	$\rho_h = 0$
$k_2 = 0.1$	$\mu_c = 0.1$	$\rho_c = 0.1$
$D_a = 0.005$	$D_h = 0.2$	

Activator-Substrate		
$\sigma_a = 0.01$	$\mu_a = 0.01$	$\rho_a = 0$
$\sigma_s = 0.02$	$\mu_s = 0$	$\rho_s = 0.02$
$D_a = 0.008$	$D_s = 0.2$	$k_s = 0.01$

Table 1: Parameters used in the experiments

We choose the diffusion coefficients D_a for the activator such that the average number of peaks obtained, and their average spacing, is approximately the same in both models, such that they can be compared.

We simulate both systems on a regular grid of 32x32 cells, using an integration timestep of $dt = 0.1$. Two scenarios are tested for each model: with and without perturbation. In the scenario without perturbation, the simulation runs without interference until it finishes at 10K simulation seconds. In the perturbed scenario, at $t = 4000s$, after the system has reached a stable pattern, perturbation events are are introduced every 1000 seconds. Each perturbation event happens as follows: 50% of the existing peaks are selected at random for disruption. If selected, a peak loses 90% of its activator concentration, and the same percentage is removed from the Moore neighborhood (8 surrounding cells) around the peak. This simulates severe disruptions, such those caused by mechanically removing chemicals, or by damaging patches of processors in amorphous computers.

A peak is a point with maximum activator concentration, i.e. the local concentration at location (x, y) is higher than all the concentrations on the Von Neumann neighborhood (north-south-east-west cells) around the peak. Moreover

[3] `www.spiderland.org`

the concentration at the peak must be above a threshold for it to be considered as a cluster head. In this evaluation study we consider only the peaks elected as cluster heads, therefore we use the terms peak and cluster head interchangeably. The peak concentration threshold is $a_{min} = 3.0$ for the activator-inhibitor model, and $a_{min} = 2.0$ for the activator substrate model.

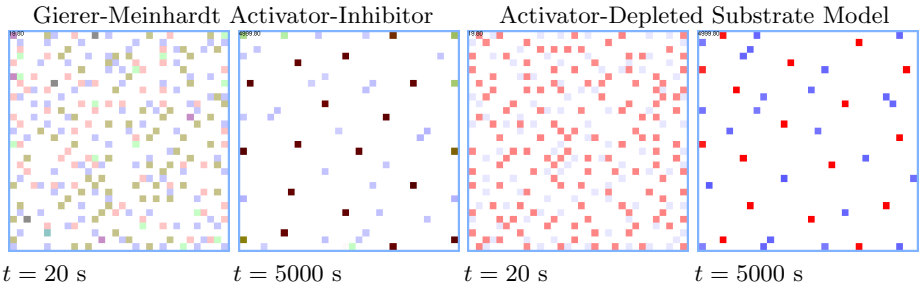

Fig. 4: Cluster head election example

Figure 4 shows an example of the process of electing activator peaks as cluster heads using the algorithm. At the beginning of the simulation ($t = 20$s) there are only very low peaks (represented by the light shaded spots) which are not elected because they are below the threshold. At $t = 5000$ seconds we can clearly see the elected peaks, indicated by brown spots in the first model, and red spots in the second. The blue spots indicate catalyst and substrate peaks which play no function as cluster heads.

5 Results

The performance of each algorithm is measured by the average distance between nearest peaks, the total number of elected peaks, and the number of cells that are served by a peak. The average distance tells the average spacing among peaks, and the number of cells that are served measures the number of cells that are located at a distance shorter than a threshold of the nearest peak, i.e. they can receive a service from this peak, such as the aggregation of some sensor information. We calculate the average distance between nearest peaks by looking at the four nearest peaks of each peak, and calculating the average of this distance for all peaks.

Figure 5 shows the average distance between nearest peaks (errorbars indicate the standard deviation). We can see that the distance remains stable when there are no disruptions. Under perturbations, the activator-inhibitor model is less stable, presenting bigger fluctuations than the activator-substrate model. Note however, that while the distance in the activator-inhibitor model remains totally constant in the absence of perturbations, in the activator-substrate model this distance fluctuates slightly, even in the absence of perturbations. This indicates that peaks are constantly moving a bit, as the underlying spots merge, grow and divide. This can be more easily seen in Figure 6 which shows the number

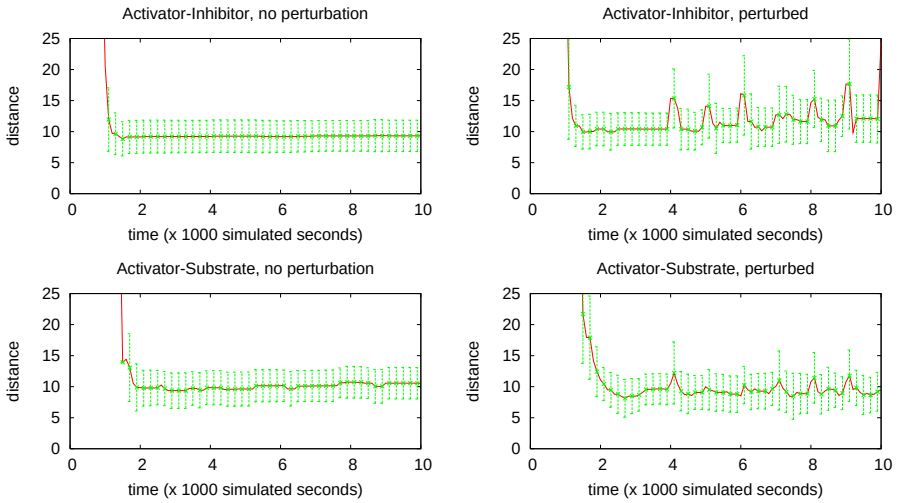

Fig. 5: Average distance between nearest peaks

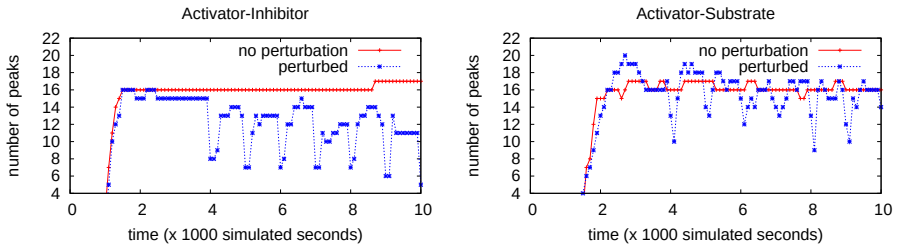

Fig. 6: Number of peaks elected as cluster heads

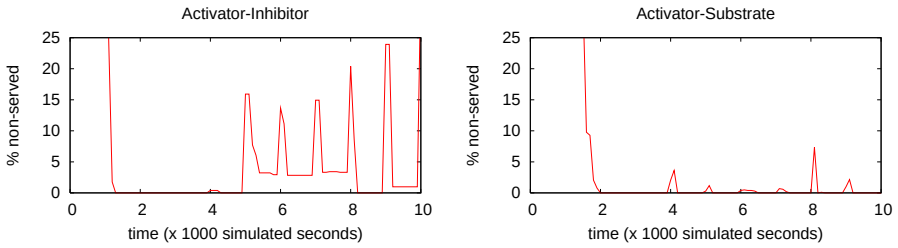

Fig. 7: Percentage of non-served cells in both models, under perturbation

of peaks elected as cluster heads. Indeed, this behavior can be easily observed when watching an animation of the activator-substrate system.

Figure 7 shows the number of cells that are at a distance bigger than $d_{max} = 10$ cells, such that they do not receive service from any nearby peak. Here we can clearly see that, under perturbation, the activator-inhibitor model leaves a larger number of cells without service than the activator-substrate model, although the average peak spacing (according to Fig. 5) is similar in both cases.

Note that, because it involves less chemicals and less reactions, the activator-substrate model is faster to compute: the simulations of the activator-inhibitor model take about 30% longer.

6 Conclusions

Activation-inhibition models have been used as models of distributed computation, to solve coordination problems such as the placement of cluster heads and the formation of content delivery highways. However, their parametrization is not simple, and performance trade-offs have to be faced.

The results reported in this paper can serve as guidelines in the design of robust algorithms based on spot patterns obtained via activation-inhibition. Two variants were evaluated, one based on an inhibitor that consumes a catalyst necessary for the activator to grow, and another one based on the depletion of a substrate also needed for activator growth.

Our results show that there is a trade-off between the stability but potentially slow response to perturbations in the activator-inhibitor model, and on the other hand, the fast response to perturbations at the cost of slowly "moving peaks" in the activator-substrate model. Therefore the first model is more appropriate in situations where, once the pattern is formed, it is not supposed to change often. While the latter is useful in more dynamic situations where frequent changes are expected, and the system should constantly react to them by quickly reconfiguring itself to a new valid configuration.

One might ask whether our results could be mere artifacts of our particular chemical implementations of both models. There might be other solutions leading to sets of reactions that do not suffer from the catalyst depletion problem found in our chemical solution for the Gierer-Meinhardt model. And there might be other solutions to the activator-substrate, or other parameter ranges where the peaks are more static. Nevertheless, we believe that our results are fairly representative of the general characteristics of both models.

As future work, a stochastic simulation of the system in larger and irregular amorphous topologies is necessary. Moreover, it would be useful to evaluate other reaction-diffusion approaches and their robustness when used as an engineering tool. It would also be interesting to study their behavior and performance in combination with other morphogenetic mechanisms. Another interesting topic for future work is to investigate the automatic evolution of reaction networks leading to the desired patterns.

Acknowledgments. This work was supported by the European Union through the BIONETS Project EU-IST-FET-SAC-FP6-027748, `www.bionets.eu`. It was performed when the first author was with the University of Basel, Switzerland. The authors would like to thank David Lowe (University of Technology Sydney, Australia) for the enticing discussions that motivated this work.

References

1. Turing, A.M.: The chemical basis of morphogenesis. Philosophical Transactions of the Royal Society of London **B 327** (1952) 37–72
2. Bar-Yam, Y.: Dynamics of Complex Systems. Westview Press (2003)
3. Meinhardt, H.: Models of biological pattern formation. Academic Press, London, UK (1982)
4. Murray, J.D.: Mathematical Biology: Spatial models and biomedical applications. Springer (2003) Volume 2 of Mathematical Biology.
5. Deutsch, A., Dormann, S.: Cellular automaton modeling of biological pattern formation: characterization, applications, and analysis. Birkhauser (2005)
6. Koch, A.J., Meinhardt, H.: Biological pattern formation: from basic mechanisms to complex structures. Reviews of Modern Physics **66**(4) (October 1994)
7. Abelson, H., et al.: Amorphous computing. Communications of the ACM **43** (May 2000)
8. Durvy, M., Thiran, P.: Reaction-diffusion based transmission patterns for ad hoc networks. In: INFOCOM. (2005) 2195–2205
9. Neglia, G., Reina, G.: Evaluating activator-inhibitor mechanisms for sensors coordination. In: Proc. Bionetics, Budapest, Hungary, ICST (2007)
10. Lowe, D., Miorandi, D., Gomez, K.: Activation-inhibition-based data highways for wireless sensor networks. In: Proc. Bionetics, Avignon, France, ICST (2009)
11. Yoshida, A., Aoki, K., Araki, S.: Cooperative control based on reaction-diffusion equation for surveillance system. In: KES (3). (2005) 533–539
12. Hyodo, K., Wakamiya, N., Murata, M.: Reaction-diffusion based autonomous control of camera sensor networks. In: Proc. Bionetics, Budapest, Hungary (2007)
13. Yu, J.Y., Chong, P.H.J.: A survey of clustering schemes for mobile ad hoc networks. IEEE Communications Surveys and Tutorials **7** (2005) 32–48
14. Erciyes, K., et al.: Graph theoretic clustering algorithms in mobile ad hoc networks and wireless sensor networks. Appl. Comput. Math. **6** (2007) 162–180
15. Soro, S., Heinzelman, W.B.: Cluster Head Election Techniques for Coverage Preservation in Wireless Sensor Networks. Ad Hoc Networks **7** (2009) 955–972
16. Dittrich, P., Ziegler, J., Banzhaf, W.: Artificial Chemistries – A Review. Artificial Life **7**(3) (2001) 225–275
17. Dittrich, P.: Chemical Computing. In: Unconventional Programming Paradigms (UPP 2004), Springer LNCS 3566. (2005) 19–32
18. Adamatzky, A., Costello, B.D.L., Asai, T.: Reaction-Diffusion Computers. Elsevier Science Inc., New York, NY, USA (2005)
19. Atkins, P., de Paula, J.: Physical Chemistry. Oxford University Press (2002)
20. Deckard, A., Sauro, H.M.: Preliminary Studies on the In Silico Evolution of Biochemical Networks. ChemBioChem **5**(10) (2004) 1423–1431
21. Dormann, S.: Pattern Formation in Cellular Automaton Models. PhD thesis, University of Osnabrück, Dept. of Mathematics/Computer Science (2000)
22. Pearson, J.E.: Complex patterns in a simple system. Science **261**(5118) (July 1993) 189– 192